

Advanced chalcogenide Ga₂S₃ coatings for reducing reflective loss and boosting efficiency in silicon photovoltaics

R. M. Reddy ^a, J. A. Prakash ^b, A. Tonk ^c, S. Karvendhan ^d, G. Sivaraman ^e,
D. K. Patel ^f, S. P. Dillibabu ^g, S. Karthikeyan ^{h,*}, T. Thirugnanasambandham ⁱ

^a Department of Mechanical Engineering, G.Pulla Reddy Engineering College, Kurnool, Andhrapradesh

^b Department of Aeronautical Engineering, Nehru Institute of Engineering and Technology, Coimbatore, Tamil Nadu

^c Department of Multidisciplinary Engineering, The NorthCap University, Gurugram

^d Department of Mechanical Engineering, Velalar College of Engineering and Technology, Erode

^e Department of Mechanical Engineering, Sona College of Technology

^f Department Mechanical Engineering, Sardar Patel College of Engineering

^g Department of Mechanical Engineering, Vel Tech Rangarajan Dr. Sagunthala R&D Institute of Science and Technology, Avadi, Chennai, Tamil Nadu, 600062

^h Department of Mechanical Engineering, Erode Sengunthar Engineering College, Perundurai, 638057, India

ⁱ Department of Mechanical Engineering, Saveetha School of Engineering, Saveetha Institute of Medical and Technical Sciences (SIMATS), Saveetha University, Chennai 602105, Tamil Nadu

The current situation necessitates advancements in renewable energy as an alternative for conventional energy sources. Reflection loss in solar cells is a contributing factor to diminish the power conversion efficiency, which can be reduced by employing antireflective coatings. The current investigation focuses on improvement in photocurrent generation of monocrystalline silicon solar cells by employing Gallium sulfide (Ga₂S₃) as anti-reflective coatings (ARC). The RF sputter coating method has been used for Ga₂S₃ deposition at different coating durations (10, 20, 30, and 40 minutes). The transmittance, reflectance, I-V characteristics, electrical properties, and thermal behaviour of the Ga₂S₃ coatings on m-Si cells were analysed to determine the influence of the coatings. The incorporation of Ga₂S₃ led to enhanced power conversion efficiencies (PCEs) from the 16.38% to 21.80% under open conditions and from 18.58% to 24.33% under closed conditions. The Ga₂S₃ coating thickness for the GS3 sample was measured at 1.440 µm using FESEM. The minimum optical reflectance of 6.56% and maximum transmittance of 93.44% were achieved after 30 minutes of coating (GS3) within the 300 to 1200 nm wavelength range. The minimum electrical resistivity of a GS3 coated sample was measured as 5.33×10⁻³ Ω-cm. Ga₂S₃ coatings serve to reduce reflected losses and improve surface passivation.

(Received June 25, 2025; Accepted September 15, 2025)

Keywords: m-Si solar cells, Anti reflection coating, Reflection loss, Power conversation efficiency and I-V characteristics

1. Introduction

Fossil fuels are essential for generating energy, comprising more than 80% of worldwide primary energy usage as of 2022. Currently, over 80% power is generated by conventional petroleum-based oils, natural gas and coal. This lead to release of massive quantities of toxic gasses and particulates, such as carbon dioxide, sulfur dioxide and nitric oxide, lead to environmental

* Corresponding author: karthiksamynathan@gmail.com

<https://doi.org/10.15251/CL.2025.229.797>

pollution and global warming [1]. The alternative sources of energy, such as solar power, wind power, hydropower, biomass, etc., are among the possibilities. Solar power represents renewable energy, serving as a cost-free and environmentally sustainable energy source [2]. The increase in the worldwide population has resulted in increased demand for renewable sources of energy. The usage of clean energy to replace traditional fossil fuels is now the prevailing energy supply trend. This is because renewable energies pose no risk to the environment. Numerous investigation projects have investigated renewable energy sources and their environmental effects [3-5]. The phenomenon known as photoelectric effect demonstrates that solar cells can convert collected light into electricity. Currently, Si cells provide superior productivity and stability compared to prior generation of solar cells [6]. A prevalent solar module employs a silicon as a base material, due to its natural availability, satisfactory PCE, and advanced technological development in this field [7].

Crystalline silicon solar panels are fundamental to photovoltaic technology, and their performance is greatly affected by the application of antireflection coatings (ARCs). Based on their availability, cost, functionality and crystallinity, solar cells were classified as either mono or polycrystalline. Monocrystalline silicon cells have a singular continuous crystal structure and are known for their high efficiency. Monocrystalline cells often exhibit lower efficiency (about 15-17%) compared to polycrystalline cells. They are manufactured by melting silicon and casting it into molds, representing a more economical manufacturing method. The reflection loss significantly affects the photocurrent output in addition to several losses [8]. Silicon possesses a high refractive index (~ 3.5 at 600 nm), resulting in considerable reflection losses at its surface. When light strikes bare silicon, around 30–35% is reflected, hence diminishing the efficiency of the PV. The increased reflection on the upper exterior surface of the PV panels reduce the PCE which in turn affects the absorbance [9]. When reflection increases, substantial fraction of photovoltaic power is wasted or reflected. In migrate reflection issues, the antireflective coating is employed. Antireflective surface coating is well known technique which significantly improves the efficiency by reducing the surface reflection [10].

The reflectance can be decreased by texturing the upper cell substrate that receives light and by employing antireflective thin film coating [11]. For ARC, highly transparent materials such as TiO_2 , SiO_2 , Si_3N_4 , Ta_2O_5 , Al_2O_3 , and $\text{SiO}_2\text{--TiO}_2$ can be used to increase the efficiency [12]. The antireflective coating technique seeks to attain near-zero reflection on silicon solar cells through the application of multilayers of metal oxides, optimizing layer thickness to facilities destructive interference, therefore markedly diminishing reflection loss and improving quantum efficiency [13]. Currently, there are two primary approaches to attain the antireflection effect, one involves the deposition of thin films including a single, double, and multi-layer films on the substrate while the other employs graded refractive index (GRIN) coatings utilizing porous and nanostructured arrays such as moth-eye structures [14, 15]. The dual layer ARCs offers more advantages than both single and multilayer ARCs [16]. Only a limited number of materials offer a suitable refractive index (generally $\sim 1.3\text{--}1.5$) and sufficient endurance for antireflective single layer coatings. Certain single-layer materials may deteriorate over time when subjected to ultraviolet radiation, humidity, or fluctuations in temperature. A double layer coating enhances optical transmission resulting in less reflection and increased sunlight absorption into the solar cell. Khuram Ali et. al [17] investigated single layer silicon dioxide and blended $\text{SiO}_2\text{--TiO}_2$ on monocrystalline silicon solar cell as an antireflective coatings by employing RF sputter deposition. The reflectance of SLAR (SiO_2) and DLAR ($\text{SiO}_2/\text{TiO}_2$) coatings were analysed to be 15 and 7%, respectively. The PCE of silicon solar cell is 2.8%, SLAR is 4.5% and DLAR is 6.2%. The decrease in reflective losses is based upon the coating quality which is determined by factors like the number of layers, coating thickness, and coating technique [18, 19].

High-quality anti-reflection film coatings are typically manufactured using vacuum-dependent techniques, comprising chemical vapor deposition, thermal evaporation, and plasma-enhanced CVD [20]. Moreover, the majority of these techniques are executed under controlled atmospheric conditions. The thin film anti-reflection coatings were applied by various deposition processes, including dip coating, sol-gel procedure, blade coating, spin coating, sputter coating and electro-spraying [21]. Power-based materials can be transformed into pellets and then utilized in the sputter deposition process. This technique offers several advantages, including excellent film adhesion, precise thickness control, and the ability to deposit coatings on complex substrate

geometries. Simultaneously, a uniform and adherent thin film can be achieved through the sputter coating process by optimizing parameters such as target power, gas pressure, substrate distance, and deposition time.

Gallium sulfide (Ga_2S_3) is being investigated as a suitable material for antireflective coatings on PV cells caused to its broad bandgap, increased optical transparency in the visible spectra, and appropriate refractive index for reducing surface reflection. Its excellent chemical and thermal stability, coupled with trust worthy adhesion to silicon surfaces, renders it a formidable for long-lasting and effective coatings. Research indicates that Ga_2S_3 thin films can greatly increase light transmission into solar cell's active layer, hence enhancing overall efficiency, particularly when incorporated into multilayer anti-reflective structures. Gallium sulfide (Ga_2S_3) is a significant semiconducting material due of its wide band gap (3.05 eV at 300 K), which provides numerous advantageous features, rendering it desirable for photoelectric devices, electrical sensors, and nonlinear optical applications. Numerous synthetic way of manufacture have been documented for the production of gallium sulfide [22].

This research involves the application of antireflective Ga_2S_3 on the silicon solar cell using the sputter coating process. The coating was conducted at several coating intervals i.e. 10 minutes (GS1), 20 minutes (GS2), 30 minutes (GS3) and 40 minutes (GS4). Transmittance, reflectance, I-V characteristics, coating morphology and temperature behavior of Ga_2S_3 coating applied to solar cells are analyzed. The ARC deposited samples are examined in open sunlight and controlled solar module setup. The entire coating process is provided in flow chart (Fig.1).

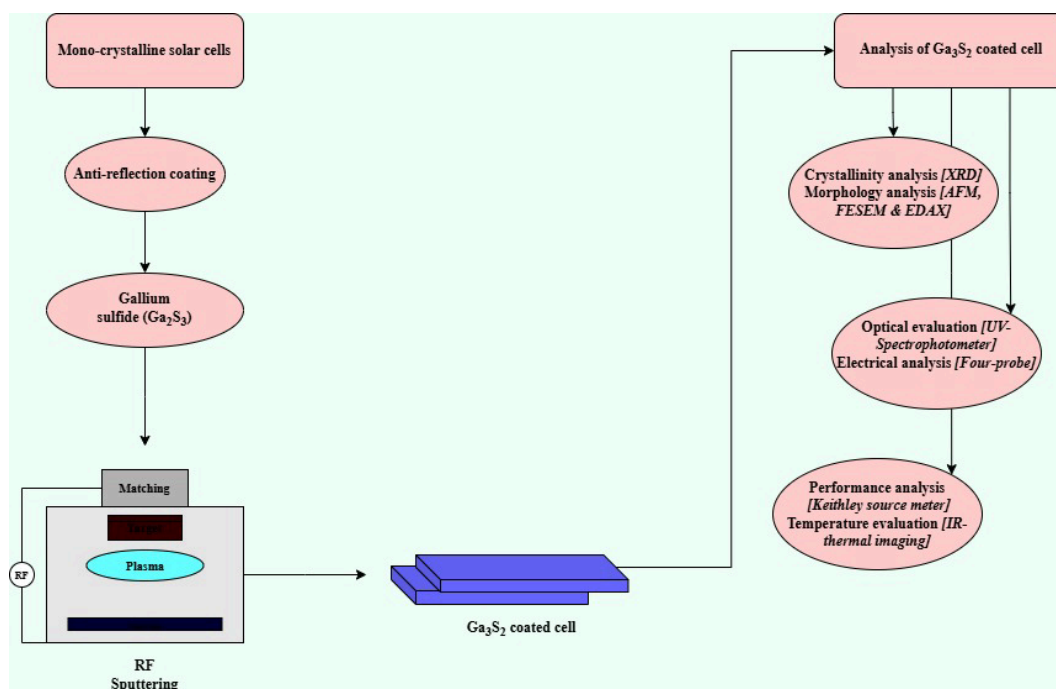


Fig. 1. Overview of Ga_2S_3 coating process.

2. Experimental techniques

2.1. Materials

The Ga_2S_3 utilized for ARC deposition method was obtained from Sigma Aldrich. The monocrystalline silicon solar cell measuring 52 mm length and 38 mm breadth was obtained from Vikram Solar, India.

2.2. Sputter deposition of Ga_2S_3

Ga_2S_3 have been applied on the monocrystalline Si cells by RF sputter deposition. The external layer of the silicon solar cell was cleansed using an ultrasonic cleaner and methanol, acetone and de-ionized water in preparation for insertion into the target holder. The mechanically pelletized pure Ga_2S_3 was separately positioned in a substrate holder for deposition. Before depositing Ga_2S_3 on the solar cell surface, a 3-minute pre-sputtering procedure was conducted. Subsequently, $\text{C}_2\text{H}_5\text{OH}$ was utilized to purify the target surface to eliminate contaminants. The sputtering process was performed to deposit Ga_2S_3 antireflection coating at various durations of 10 - 40 mins.

2.3. Characterization methods

The X'Pert PRO analyzer was enhanced X-ray diffraction investigations of the materials, illuminating their crystal structure and structural properties. The roughness of the ARC deposited cells was examined by atomic force microscopy (AFM). The morphological image of various Ga_2S_3 samples were analyzed by a Field Emission Scanning Electron Microscopy (FESEM). An energy-dispersive X-ray (EDX) spectrometer was employed to investigate the chemical composition of coated specimens. The optical study of ARC specimens were performed using UV spectroscopy. The current-voltage (IV) properties of ARC cells were evaluated using a Keithley 2450 instrument. Thermal analysis of ARC cells was performed utilizing infrared thermography.

3. Findings and discussion

The XRD technique enables the examination of crystalline structural properties of Ga_2S_3 coated cells as depicted in fig. 2. The observation of Si peaks in all the Ga_2S_3 deposited cells indicates that the coated cells consist of crystalline silicon. The obtained XRD peak intensities align with the standard JCPDS cards: 48-1432 (Ga_2S_3). The crystal structure of Ga_2S_3 nanoparticles was tetrahedral as confirmed by XRD data. The obtained Miller indices (001), (100), (010), (111), (112), (220), (311), (100) and (110) are accurately indexed according to the Ga_2S_3 structure.

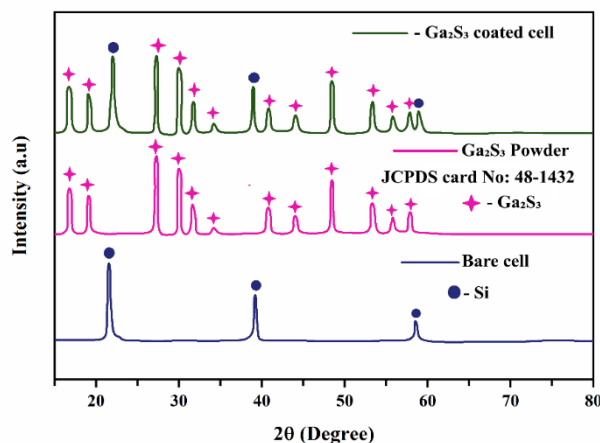


Fig. 2. X-ray diffraction evaluation of Ga_2S_3 deposited cells.

Fig. 3 shows the surface topology and roughness of ARC cells from AFM analysis. The average roughness values were evaluated by the tapping method. In tapping mode, a $20\ \mu\text{m} \times 20\ \mu\text{m}$ region was analysed to calculate the roughness of Ga_2S_3 film-coated photovoltaic cells. The measured surface roughness of Ga_2S_3 coated samples such as GS1, GS2, GS3 and GS4 were 94, 117, 126 and 131 nm, respectively. As seen increase in coating time leads to increase the surface roughness. When light reaches a rough surface, it spreads out, developing the optical path longer inside the cell and reducing reflected losses [23].

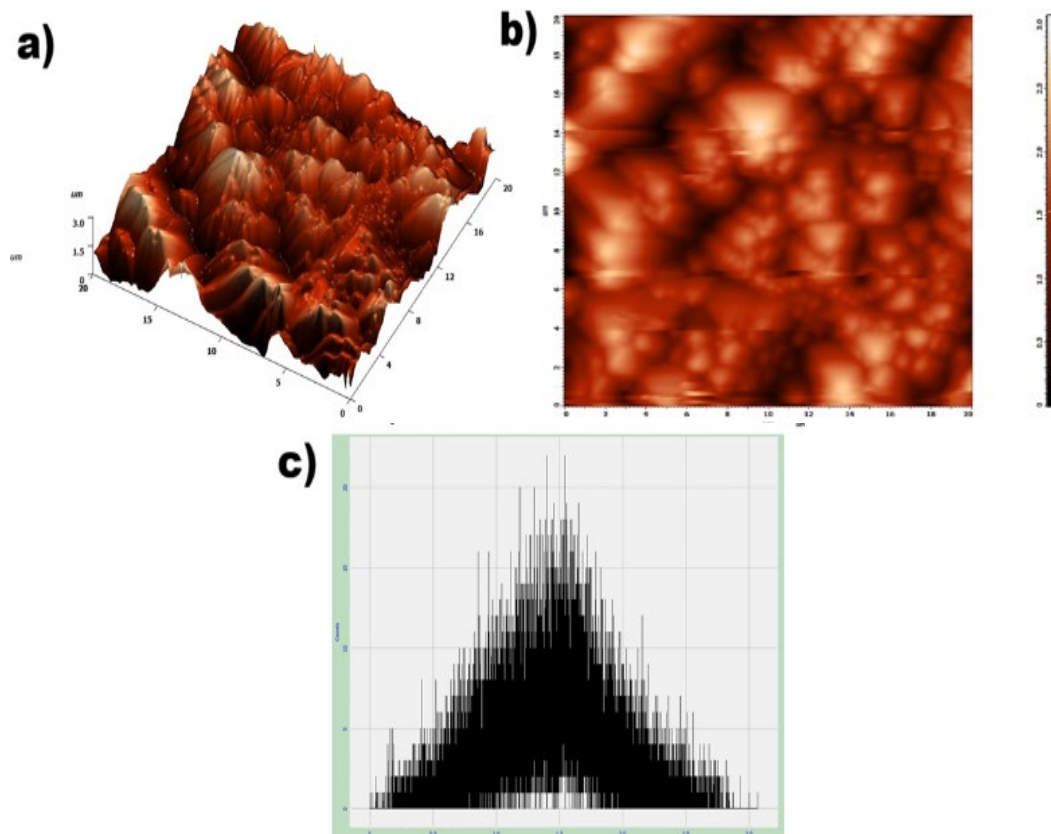


Fig. 3. Surface roughness of Ga_2S_3 deposited cells.

FESEM is utilized to analyze the microstructure and thickness of Ga_2S_3 sample as seen in fig. 4a and 4b. As seen, there exists uniformity in the deposition of ARC material on the surface of m-Si cells. A uniform distribution of coating thickness in antireflective (AR) layers is crucial for optimizing the PCE of silicon solar cells, as it directly influences optical interference, reflection reduction, and device dependability [24]. As seen, the coating thickness keeps going up as the coating time is increased. Fig. 4(b) shows FESEM cross-sectional image GS3 coatings thickness of $1.440\ \mu\text{m}$. The elemental constituents of Ga_2S_3 coated solar cell were confirmed using EDAX analysis. Fig. 5 displays the presence of several components in coating of Ga_2S_3 , containing Ga, Si and Se. There was a significant quantity of Si peaks, because of the utilization of monocrystalline silicon cells.

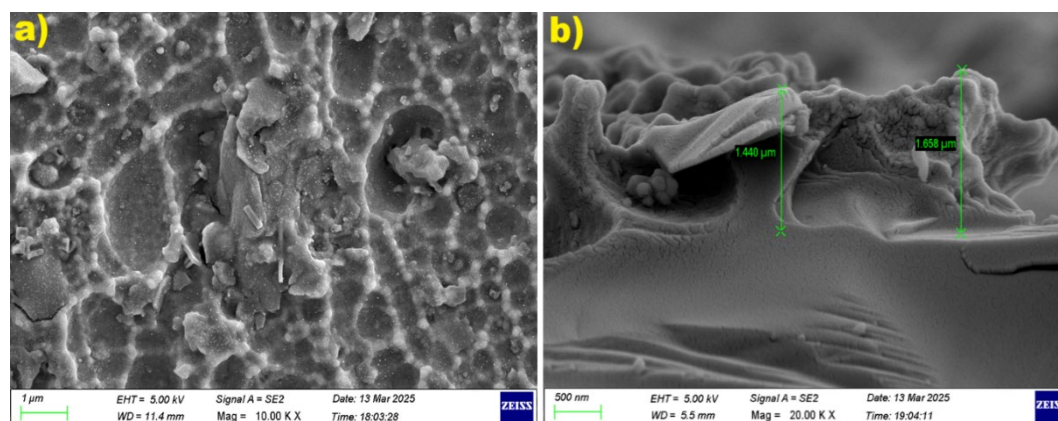


Fig. 4. FESEM: (a) Coating morphology (b) Coating thickness of GS3 coated cell.

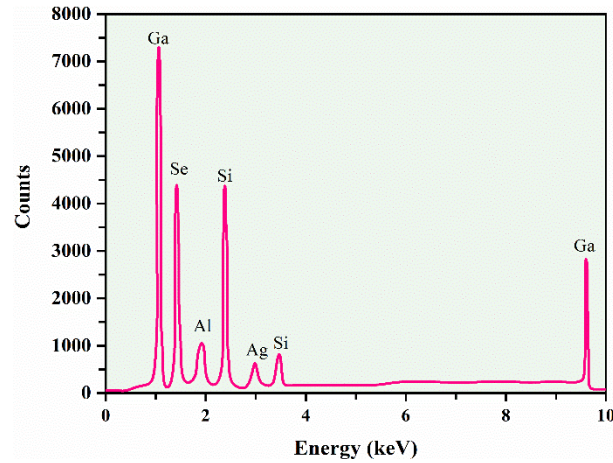


Fig. 5. Elemental composition of Ga_2S_3 coated Si solar cell.

Fig. 6 illustrates the optical transmittance and reflectance of Ga_2S_3 deposited samples. The transmittance of Ga_2S_3 coated and uncoated cell was observed across the visible spectrum (300nm-1200 nm). From Table 1, it is evident that the Ga_2S_3 deposition at GS3 minutes attains the highest transmittance of 93.4 % among all the samples analysed. The transmittance values for samples GS1 to GS3, exhibit a progressive enhancement. While coating duration is increased to 40 mins at GS4 it leads to increased reflectance (16.38%) and decreased transmittance (83.62%). The investigation reveals that modifying the coating thickness was essential for optimizing cell performance, diminishing reflection and augmenting transmittance. GS3 coated solar cell exhibited a 79.57% decrease in reflectance of GS3 to bare solar cells, attributed to the improved passivity provided by the Ga_2S_3 layer. The increased surface texture enables incoming light to become captured in gap, leading to significant internal reflection that considerably diminishes reflectance loss [25].

Table 1. Optical properties of bare cell and various Ga_2S_3 coated solar cell.

Samples	Transmittance (%)	Reflectance (%)
Bare cell	67.89	32.11
GS1	76.05	23.95
GS2	78.76	21.24
GS3	93.44	6.56
GS4	83.62	16.38

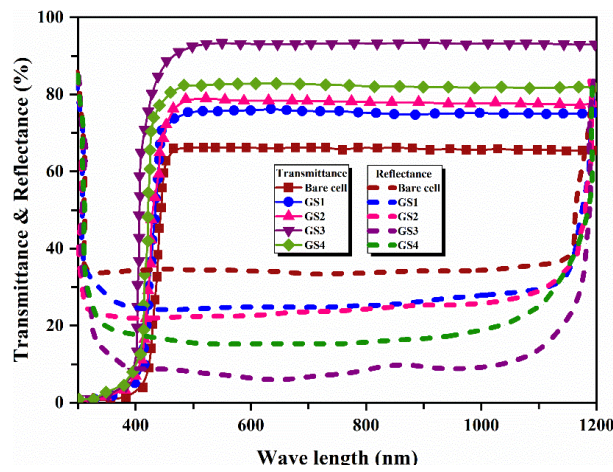


Fig. 6. Transmittance and reflectance of bare cell and Ga_2S_3 deposited cells.

The electrical resistivity, hall mobility and carrier concentration of solar cell specimens were analyzed utilizing a four-probe technique, as seen in fig. 7. The GS3 coating on the solar cell has a low electrical resistance of $5.33 \times 10^{-3} \Omega \text{ cm}$. The uncoated sample demonstrates a maximum resistance of $8.15 \times 10^{-3} \Omega \text{ cm}$. The resistance diminishes with improved light transparency and carrier concentration, as illustrated in Table 2. The Ga_2S_3 (GS3) coating achieves the highest hall mobility ($15.43 \text{ cm}^2 \text{ V}^{-1} \text{ s}^{-1}$) and carrier concentration of $37.09 \times 10^{20} \text{ cm}^{-3}$. The utilization of Ga_2S_3 material with diminished grain boundaries significantly enhances the exciton production and recombination [26]. Exciton mobilization grows with the augmentation of photocurrent generation and light intensity.

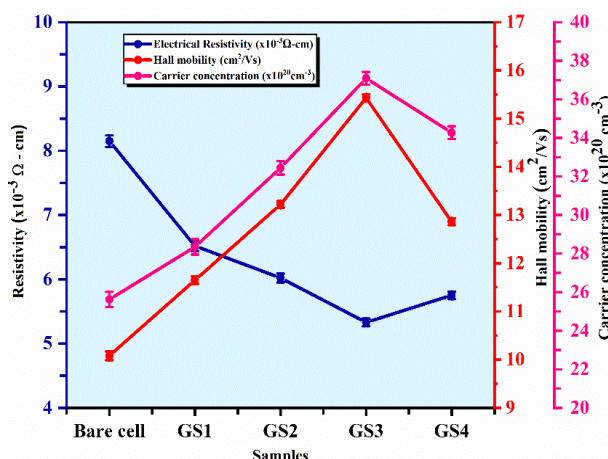


Fig. 7. Electrical features of bare and Ga_2S_3 deposited samples.

Table 2. Electrical properties of bare cell and various Ga_2S_3 coated solar cell.

Specimen	Resistivity $\times 10^{-3}$ ($\Omega \cdot \text{cm}$)	Carrier concentration $\times 10^{20}$ (cm^{-3})	Hall mobility ($\text{cm}^2 \text{ V}^{-1} \text{ s}^{-1}$)
Bare cell	8.15	25.62	10.08
GS1	6.52	28.35	11.65
GS2	6.02	32.44	13.22
GS3	5.33	37.09	15.43
GS4	5.75	34.27	12.86

Fig. 8 and Table 3 and 4 illustrates the I-V characteristics of bare, Ga_2S_3 GS1, GS2, GS3, and GS4 coated m-Si cells under open and closed UV radiation. The voltage and current readings are captured and plotted into an I-V profile, from which productivity may be evaluated. The uncoated sample attains a PCE of 16.38% and 18.58%, with the parameters: $J_{\text{SC}} = 35.55 \text{ mA/cm}^2$ and 38.99 mA/cm^2 , $V_{\text{OC}} = 0.631 \text{ V}$ and 0.662 V , $\text{FF} = 73\%$ and 72% under open and controlled environments respectively. The GS3 coated silicon solar cells have enhanced photocurrent production, attaining a PCE of 21.80% with $J_{\text{SC}} = 41.79 \text{ mA/cm}^2$, $V_{\text{OC}} = 0.652 \text{ V}$, and $\text{FF} = 78\%$ in open condition. It is also seen that, GS3 sample has the highest PCE of 24.33%, J_{SC} of 44.56 mA/cm^2 , V_{OC} of 0.7 V , and FF of 82% in closed conditions. An increase in J_{SC} and V_{OC} results in an enhancement of PCE from 16.38% to 21.80% under open conditions and from 18.58% to 24.33% under closed conditions. The enhancement of fill factor results in improved current production.

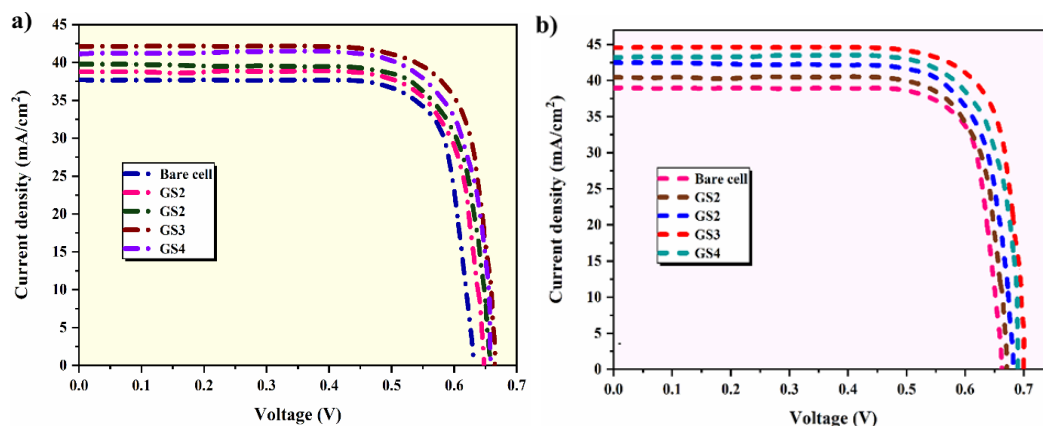


Fig. 8. Current-voltage properties of bare and Ga_2S_3 cells under (a) open and (b) closed condition.

Fig. 9 illustrates the thermal analysis of (a) bare, (b) GS1, (c) GS2, (d) GS3, and (e) GS4 in open and closed system conditions to evaluate surface temperature. The efficiency of solar cells diminishes as temperature rises. The infrared (IR) imaging approach is employed to ascertain the operational temperature of various coated solar cells. The findings reveal that GS3 coated solar cells show minimum temperature of $56.4^{\circ}C$ (closed) and $36.5^{\circ}C$ (open) which is lower than other samples. The enhanced light scattering elevates the thermal transfer of solar cells, hence diminishing the transparency of the anti-reflective coating. consequently, a lower surface temperature improves the efficiency of m-Si cells [27]. Thus, it is evident that the Ga_2S_3 layer functioned as an exceptional anti-reflective coating material for enhancing PCE.

Table 3. *I-V* properties of bare and various Ga_2S_3 deposited samples in solar light.

Samples	J_{sc} (mA/cm ²)	V_{oc} (V)	FF (%)	PCE (%)
Bare cell	35.55	0.631	71	16.38
GS1	37.73	0.642	74	18.17
GS2	39.43	0.65	76	19.73
GS3	41.79	0.652	78	21.80
GS4	40.32	0.651	75	20.47

Table 4. *I-V* properties of bare and various Ga_2S_3 deposited samples under stimulated condition.

Samples	J_{sc} (mA/cm ²)	V_{oc} (V)	FF (%)	PCE (%)
Bare cell	38.99	0.662	73	18.58
GS1	40.45	0.671	76	20.09
GS2	42.46	0.682	78	21.72
GS3	44.56	0.7	82	24.33
GS4	43.17	0.69	79	22.64

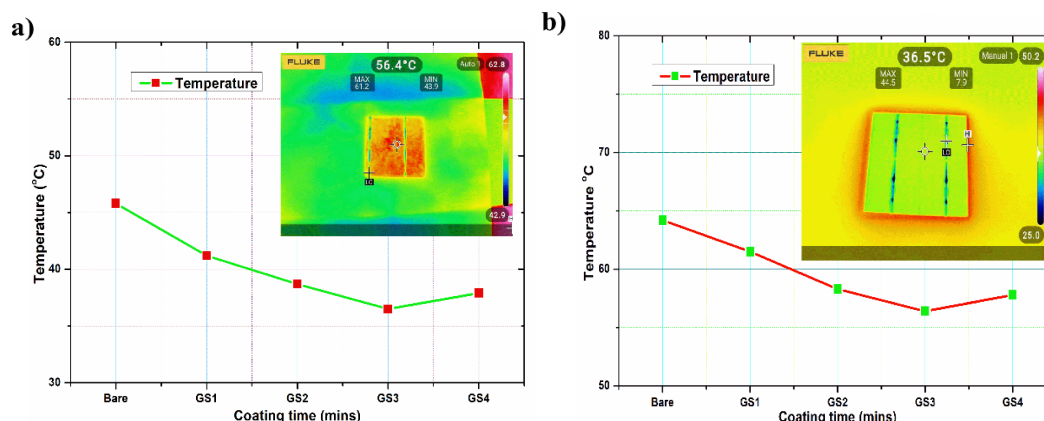


Fig. 9. IR thermal imaging of GS3 coated cell under (a) open and (b) closed condition.

4. Conclusion

The Ga_2S_3 coated material was applied to the solar cell surface using the sputter coating process. The miller indices (001), (100), (010), (111), (112), (220), (311), (100) and (110) derived from XRD data align closely with Ga_2S_3 crystal structure. The surface roughness of Ga_2S_3 sample GS1, GS2, GS3 and GS4 was measured at 94, 117, 126 and 131 nm, respectively. The FE-SEM analysis indicates cross-sectional thickness of GS3 coated solar cell is 1.440 μm . The GS3 deposited cell displays a improved transmittance of 93.44% and the minimal reflectance of 6.56% when compared to bare cells and different anti-reflective coating placed on m-Si cells. The m-Si cells with Ga_2S_3 (GS3) anti-reflective coating demonstrated enhanced PCE, reaching 21.80% and 24.33% under open and closed conditions respectively. The major improvements in the performance of Ga_2S_3 applied on Si cells may be attributed to the reconfiguration of its morphological characteristics and thermal properties.

References

- [1] G. Wei, Shanghai electric power 4), 2006); <https://doi.org/10.1049/cp:20061648>
- [2] C.-H. Park, Y.-J. Ko, J.-H. Kim, H. Hong, Energies 13(10), 2020); <https://doi.org/10.3390/en13102568>
- [3] M.K.H. Rabaiia, M.A. Abdelkareem, E.T. Sayed, K. Elsaid, K.-J. Chae, T. Wilberforce, A. Olabi, Science of The Total Environment 754(2021); <https://doi.org/10.1016/j.scitotenv.2020.141989>
- [4] R. Al Afif, B. Linke, Energy 171(2019); <https://doi.org/10.1016/j.energy.2019.01.080>
- [5] H. Al-Najjar, C. Pfeifer, R. Al Afif, H. J. El-Khozondar, Designs 4(3), 2020); <https://doi.org/10.3390/designs4030032>
- [6] J. Rath, Solar Energy Materials and Solar Cells 76(4), 2003); [https://doi.org/10.1016/S0927-0248\(02\)00258-1](https://doi.org/10.1016/S0927-0248(02)00258-1)
- [7] A. Żabnieńska-Góra, N. Khordehgah, H. Jouhara, Renewable Energy 163(2021); <https://doi.org/10.1016/j.renene.2020.10.123>
- [8] D. Chen, Solar Energy Materials and Solar Cells 68(3-4), 2001); [https://doi.org/10.1016/S0927-0248\(00\)00365-2](https://doi.org/10.1016/S0927-0248(00)00365-2)
- [9] K.T. Roro, N. Tile, B. Yalisi, M. De Gama, T. Wittes, T. Roberts, A. Forbes, 2011).
- [10] D.N. Joshi, S. Atchuta, Y.L. Reddy, A.N. Kumar, S. Sakthivel, Solar Energy Materials and Solar Cells 200(2019); <https://doi.org/10.1016/j.solmat.2019.110023>

- [11] C.-H. Sun, P. Jiang, B. Jiang, *Applied Physics Letters* 92(6), 2008);
<https://doi.org/10.1063/1.2870080>
- [12] D.-S. Wu, C.-C. Lin, C.-N. Chen, H.-H. Lee, J.-J. Huang, *Thin Solid Films* 584(2015);
<https://doi.org/10.1016/j.tsf.2015.01.042>
- [13] H. Khmissi, B. Azeza, M. Bouzidi, Z. Al-Rashidi, *Engineering, Technology & Applied Science Research* 14(3), 2024); <https://doi.org/10.48084/etasr.7375>
- [14] J.W. Leem, J.S. Yu, *Rsc Advances* 5(75), 2015); <https://doi.org/10.1039/C5RA05991G>
- [15] H.K. Raut, S.S. Dinachali, A.Y. He, V.A. Ganesh, M.S. Saifullah, J. Law, S. Ramakrishna, *Energy & Environmental Science* 6(6), 2013); <https://doi.org/10.1039/c3ee24037a>
- [16] A. Ibrahim, A. El-Amin, *International Journal of Renewable Energy Research* 2(3), 2012).
- [17] K. Ali, S.A. Khan, M.M. Jafri, *International Journal of Electrochemical Science* 9(12), 2014); [https://doi.org/10.1016/S1452-3981\(23\)11011-X](https://doi.org/10.1016/S1452-3981(23)11011-X)
- [18] A.S. Sarkın, N. Ekren, Ş. Sağlam, *Solar energy* 199(2020);
<https://doi.org/10.1016/j.solener.2020.01.084>
- [19] L. Xu, X. Li, Y. Chen, F. Xu, *Applied Surface Science* 257(9), 2011);
<https://doi.org/10.1016/j.apsusc.2010.11.170>
- [20] Z. Liang, W. Li, B. Dong, Y. Sun, H. Tang, L. Zhao, S. Wang, *Chemical Physics Letters* 716(2019); <https://doi.org/10.1016/j.cplett.2018.12.030>
- [21] P. Gu, X. Zhu, J. Li, H. Wu, D. Yang, *Journal of Materials Science: Materials in Electronics* 29(2018); <https://doi.org/10.1007/s10854-018-9599-6>
- [22] P. Hu, Y. Liu, L. Fu, L. Cao, D. Zhu, *Applied Physics A* 80(2005);
<https://doi.org/10.1007/s00339-004-3187-8>
- [23] A.H.K. Mahmoud, F.M. Korany, C. Tharwat, M. Hussein, M.A. Swillam, S.S.A. Obayya, M.F.O. Hameed, *Journal of Photonics for Energy* 10(4), 2020);
<https://doi.org/10.1117/1.JPE.10.045502>
- [24] M.M. Diop, A. Diaw, N. Mbengue, O. Ba, M. Diagne, O.A. Niasse, B. Ba, J. Sarr, *Materials Sciences and Applications* 9(08), 2018).
- [25] W. Wang, L. Qi, *Advanced Functional Materials* 29(25), 2019);
<https://doi.org/10.1002/adfm.201807275>
- [26] N. Almakayeel, G.V. Kaliyannan, R. Gunasekaran, R. Rathanasamy, *Journal of Materials Research and Technology* 2024).
- [27] A. Alshammari, E. Almatrafi, M. Rady, *Solar Energy* 273(2024);
<https://doi.org/10.1016/j.solener.2024.112545>